COUPLED CALCULATIONS OF SAS4A/SASSYS-1 AND STAR-CCM+ FOR THE SHRT-45R TEST IN EBR-II

Klaus Huber
Karlsruhe Institute of Technology (KIT)
Kaiserstrasse 12, 76131 Karlsruhe
Klaus.Huber@kit.edu

Justin W. Thomas
Nuclear Engineering Division
Argonne National Laboratory
9700 South Cass Avenue, Bldg. 208
Argonne, IL 60439-4842
Justin.Thomas@anl.gov

ABSTRACT

Many efforts are taken worldwide to extend present knowledge and enhance the capability of SFRs. One of the points of interest during R&D is nuclear safety. The Shutdown Heat Removal Tests (SHRT), performed at the Experimental Breeder Reactor-II (EBR-II) in the United States, demonstrated the passive safety response of sodium-cooled fast reactors and the potential to withstand accidents with highly unlikely initiating events. The focus of this present work is the thermal hydraulic behavior. The SHRT-45R test is taken as physical basis. The test represents an unprotected loss-of-flow accident (ULOF) scenario. The SAS4A/SASSYS-1 system thermal hydraulic (STH) code is taken to represent the primary circuit with given boundary conditions. STH codes are known to be able to calculate complex and large systems during transient behavior. Large volumes are expected to be of strong three-dimensional behavior and likely to contain phenomena like thermal stratification or thermal striping. As STH codes do not fully cover those phenomena, the cold pool is researched with Computational Fluid Dynamics (CFD). An existing coupling approach is used and extended to calculate the whole transient with the SAS4A/SASSYS-1 (STH) code coupled with the STAR-CCM+ (CFD) code. This way the strength of the STH (calculation time for large, complex systems) and CFD (three-dimensional representation) can be combined for an enhanced solution.

In this report, the SHRT-45R test case scenario is introduced shortly. Starting with a given STH model, the development of the CFD model is shown. Here, efforts have been taken to keep up the EBR-II cold pool's structural complexity as high as possible without losing calculation time out of focus. Afterwards, coupled calculation results are shown and discussed. Especially for three-dimensional flow conditions in large volumes, it is shown CFD gives better representation of the flow regime than STH standalone.

KEYWORDS
SHRT-45R, coupling, SAS4A/SASSYS-1, STAR-CCM+

1. INTRODUCTION

In sodium cooled fast reactors (SFR) of the next generation (Gen-IV) [1], the drive to reduce costs forces in the same time the structural simplification and the increase of power. Accordingly, nuclear thermal-hydraulic complexity will be increased progressively and requires state-of-the-art tools to face this challenge [2].
During the last half century, system thermal-hydraulics have been being developed to support nuclear safety and qualification procedures [3]. Their verification and validation is through extensive experimental programs that support measurements of transients – e.g. in case of water cooled systems [4]. For sodium applications especially, [5] showed the need of improvement on numerical simulation. One of these field is thermal stratification [5] and thermal striping [6] which as of now is still not fully possible to be modelled in system thermal-hydraulic scale but can be supported by system thermal-hydraulics (STH) / computational fluid dynamics (CFD) coupling.
During the 1980s, Argonne National Laboratory conducted a Shutdown Heat Removal Test (SHRT) series [7] to research inherent safety of the Experimental Breeder Reactor II (EBR-II) under which a severe unprotected loss-of-flow test (SHRT-45R) demonstrated the effectiveness of passive feedback in the EBR-II reactor. One test in that campaign of shutdown heat removal tests (SHRT) is the SHRT-45R, a simulated station blackout or unprotected loss of flow accident scenario.
The SAS4A/SASSYS-1 STH code is being developed by Argonne National Laboratory (ANL) [8]. The code capabilities reach from heat transfer, thermal-hydraulics, and neutronics behavior of either a pool-type or loop-type and will be described briefly in [3]. The cold pool is identified as large volume and yields handling of complex three-dimensional, thermal-hydraulic behavior that can be hardly approximated by a STH code. To solve this challenge, STAR-CCM+ [9] has been used as CFD code as explained in 4. The transient boundary conditions for CFD are calculated by the STH code and CFD results are returned to STH in every time step as shown in chapter 5.

2. EBR-II and the SHRT-45R transient

The Experimental Breeder Reactor II (EBR-II) had been operated over 30 years. It is a U.S. Department of Energy (DOE) facility located in Idaho and operated by Argonne National Laboratory (ANL) [10]. The first delivery of electrical power to the National Reactor Testing Station distribution grid began in August 1964. EBR-II was shut down on September 30, 1994. Initially, the objective was to verify and demonstrate a liquid metal cooled fast reactor as an electric power generating plant operating on recycled fuel. Later on, the mission was changed to support the development of uranium-plutonium mixed oxide fuel for liquid metal cooled fast breeder reactors. During the 1980s, an extensive program of safety experiments had been conducted. The SHRT test series of EBR-II was carried out between 1984 and 1986 [7].
The EBR-II reactor consists of three circuits: liquid sodium in primary and intermediate circuit and water in secondary circuit to drive the turbine/generator [11]. In the primary circuit, liquid sodium flows through the subassemblies, where it is heated, to the hot plenum. The hot plenum is connected to the Intermediate Heat Exchanger (IHX) by the so-called Z-Pipe. In the IHX, heat is transferred from primary to intermediate circuit. Cooler primary sodium then enters the cold pool, a large volume whose surface is covered by argon gas. Two identical (mechanical) pumps drive sodium from the cold pool through piping (high and low pressure piping) to the core support structure from where sodium flows again upwards through the core structure. Additionally to the two mechanical pumps in the cold pool, the primary circuit has one auxiliary pump which is an electromagnetic (EM) pump in the Z-Pipe close to the IHX inlet region. A schematic is shown in Figure 1. Additionally to the described main flow, there were identified a number of bypassing flows from the hot side to the cold pool.

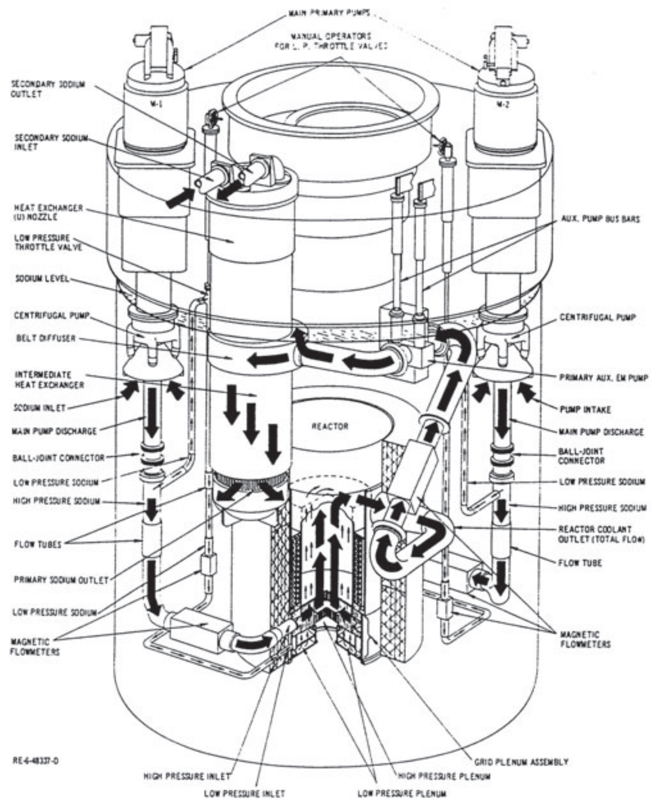

Figure 1. EBR-II primary circuit (12)

The SHRT-45R was conducted on April 3, 1986 [13], [14]. As initial condition, EBR-II was operated at full power and flow condition. Prior modifications in the plant protection system (PPS) prevented it from initiating a control rod scram before the end of the test. After reaching the initial (steady state) condition, both primary pumps and intermediate pumps were tripped for the simulation of a loss-of-flow accident (LOF). Normally, the reactor would be scrammed immediately after such an event. The prior modifications to the plant prevented this reaction, so the core still operated under full power only dependent on the effectiveness of passive feedback in the reactor. This transient condition caused a temporarily rise in in temperature to a high, but acceptable level as the reactor safely shut itself down due to total negative reactivity feedback.

The test demonstrated SFR plants can be designed in a way that natural phenomena (e.g. thermal expansion of reactor materials, natural circulation, thermal stratification) are effective design approaches in protecting the reactor against potentially adverse consequences during loss-of-flow accidents, as opposed to electromechanical system designs (e.g. control drives). In the design of SFR plants, reactivity feedbacks can be made to play a major role in protecting the reactor [14]. Being able to predict this behavior accurately is important to the licensing process of any future fast reactor design.

3. STH (SAS4A/SASSYS-1) model used

The SAS4A/SASSYS-1 STH codes are being developed at Argonne National Laboratory (ANL) for thermal, hydraulic and neutronic analysis of power and flow transients in liquid-metal-cooled nuclear reactors (LMRs) [15].

The PRIMAR-4 module (16) of SAS4A/SASSYS-1 represents the coolant flow and heat transfer in the sodium heat removal systems. Accurate representation of the sodium volumes and flow paths is essential for correctly predicting thermal inertia, heat transport, time constants, and natural circulation during a transient. Models are composed of volumes of sodium connected by one dimensional flow segments. These volumes are referred to as compressible volumes, or CVs, and may represent inlet plena, outlet plenum, pools, pipe tees, and other volumes. The PRIMAR-4 model of the EBR-II primary circuit (Figure 2) has been modelled by [17] for the case of SHRT-45R and SHRT-17.

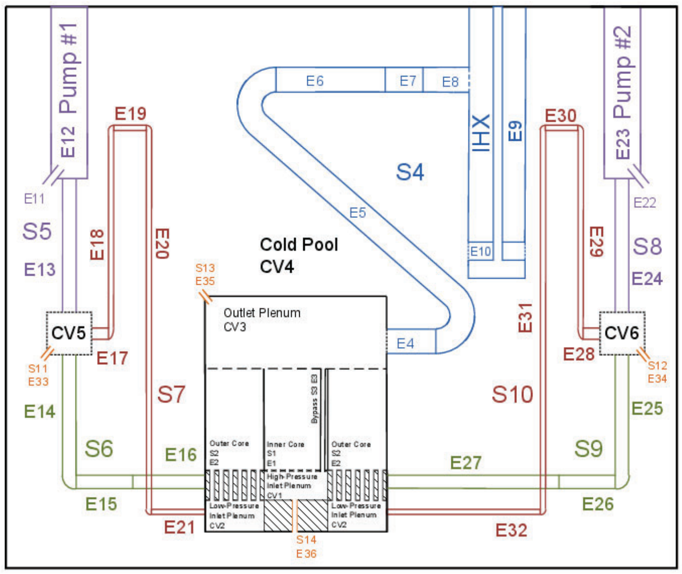

Figure 2. PRIMAR-4 Primary Sodium System Model (17)

The system model is partitioned into a number of segments. Segment 1 represents subassemblies of the outer core, Segment 2 of the inner core. Additionally, a bypass flow has been introduced (Segment 3) to take into account sodium flow in the gaps between subassemblies, the control and safety subassemblies, and flow through the grid structure, vent holes and shields. Segments 1 and 2 receive sodium from the high pressure inlet plenum (CV1) and the low pressure inlet plenum (CV2). Both segments are connected to CV3, the common outlet plenum. Sodium exits the outlet plenum into the Z-Pipe (Segment 4), which contains the auxiliary electromagnetic pump and the primary side of the Intermediate Heat Exchanger (IHX). From Segment 4 (at the IHX outlet), primary sodium enters the large volume of the cold pool (CV4). The cold pool feeds the primary sodium pumps (Segments 5 and 8) and is then discharged from the pumps downwards to either CV5 or CV6 (dependent on which pump is meant) where sodium is divided in the high pressure and low pressure inlet piping. Segment 6 and 9 model the high pressure inlet piping and are connected to the high pressure inlet plenum (CV1), Segments 7 and 10 model the low pressure piping and are connected to the low pressure inlet plenum. Segments 5-7 and Segments 8-10 are modelled identically.

Four leakage flow path are modeled by Segments 11-14. Segments 11 and 12 model the pump outlet leakage and throttle valve leakage to the cold pool. The throttle valve is part of the low-pressure inlet piping. As it is of minor influence and would also only be connected to CV4 (cold pool), it is not considered in the modelling for the SHRT-45R benchmark test. Segment 13 represents sodium leakage flow from the outlet plenum. Sodium is discharged here through the gap between reactor cover and shielding into the cold pool. Additionally, the Z-Pipe leaks sodium near the connection to the IHX. As in the case of the throttle valve, the Z-Pipe leak and the reactor cover leak are represented by one segment,

Segment 13. Segment 14 represents sodium leakage at the inlet plena, around the subassembly adapters into the cold pool.
The SAS4A/SASSYS-1 model of the EBR-II SHRT-45R benchmark test provides boundary conditions for CFD calculations of steady state of the Cold Pool and coupled calculations later on.

4. CFD modelling

The CFD model developed for the EBR-II cold pool for a coupled solution started in 2011. Reference [18] describes a preliminary CFD model and its coupled solution with SAS4A/SASSYS-1. Hence the CFD model had to be revised or substituted. In following the geometry, boundary conditions, meshing and numerical setup for CFD will be shown.
As a starting point of every CFD model, the 3D geometry is built in STAR-CCM+ 3D CAD module. As the previous geometry model of the EBR-II cold pool uses geometries from the SAS4A/SASSYS-1 model, more geometrical information from the EBR-II construction is used here. Especially the primary pumps, high and low pressure piping, intermediate heat exchanger (IHX) and Z-Pipe are modelled in more details as shown in Figure 3.

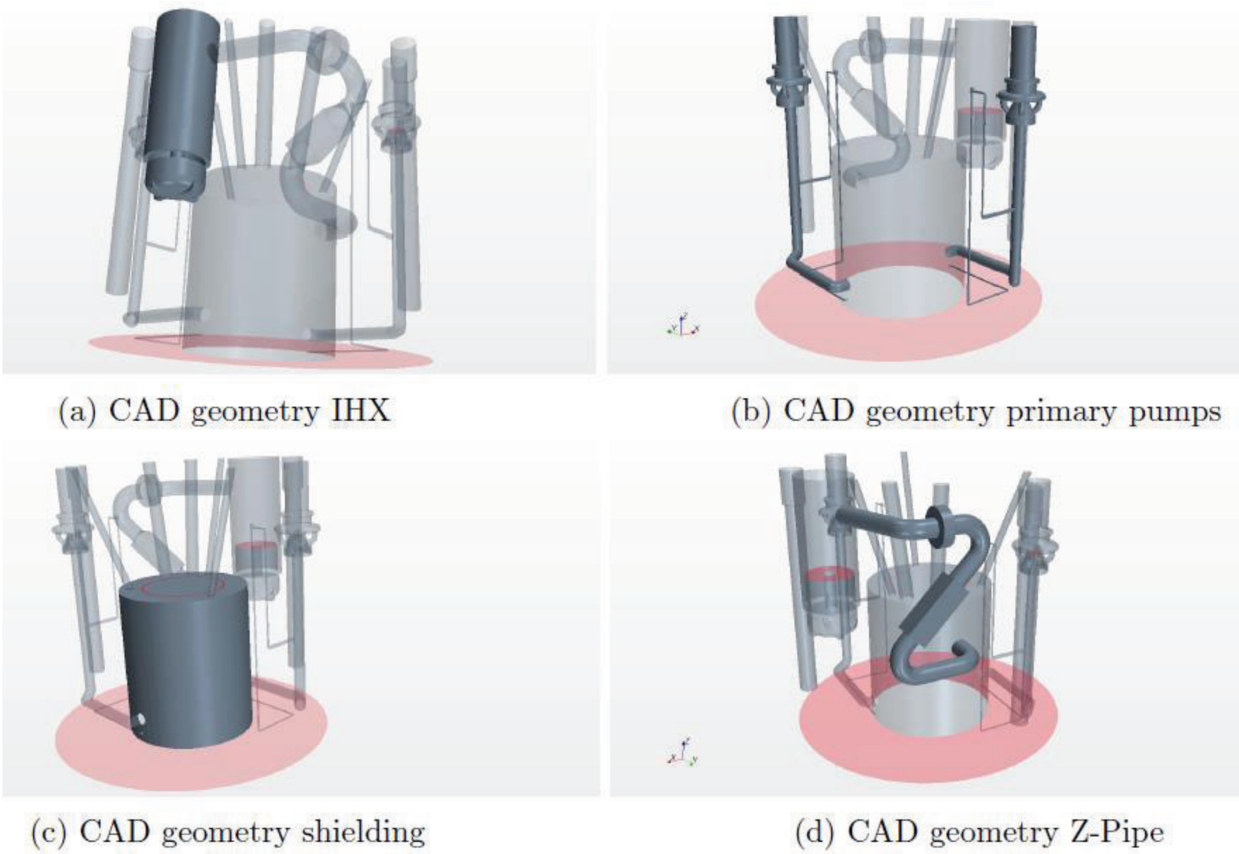

(a) CAD geometry IHX (b) CAD geometry primary pumps

(c) CAD geometry shielding (d) CAD geometry Z-Pipe

Figure 3. EBR-II geometries with STAR-CCM+ CAD modeller

Figure 3 (a) shows the IHX. It is mainly a cylindrical geometry with an annulus region within. The horizontal region at the top of the annulus region is used for inlet flow boundary definitions. The main

flow (besides leakage flows) to the cold plenum is from the IHX outlet. The boundary is defined by velocity and temperature. The geometry at the bottom of the IHX enhances the structural integrity. The two primary pumps (Figure 3 (b)) are modelled as close to the reality as information was available. However, the inlet region to the rotor within the pumps (conical region) is considered as outlet boundary condition of the volume. The shielding, illustrated in Figure 3 (c) is considered as a simple cylinder. On top of the geometry, the leakage flows from the outlet plenum is imprinted. The assumption was made, leakage from the small gap between shielding and core cover can bypass the IHX and directly enter the cold pool through an annulus region concentric on top of the core shielding. One of the more complex geometries is the Z-Pipe (see Figure 3 (d)), which has only been taken into account as construction. Some more simple geometries like the decay heat removal system, measurement arms and fixation arms have been modeled coarsely as a consequence of missing (reliable) geometry data. The described geometries do not yet have flow within and can yet be considered as wall geometries. One of the reasons why they have been modeled is the volume, they subtract form the sodium pool (fluid region).
The main fluid structure is region based meshed [9] with polyhedral cells and 3 prism layers near the wall which is sufficient for high-Reynolds turbulence models as applied later on.

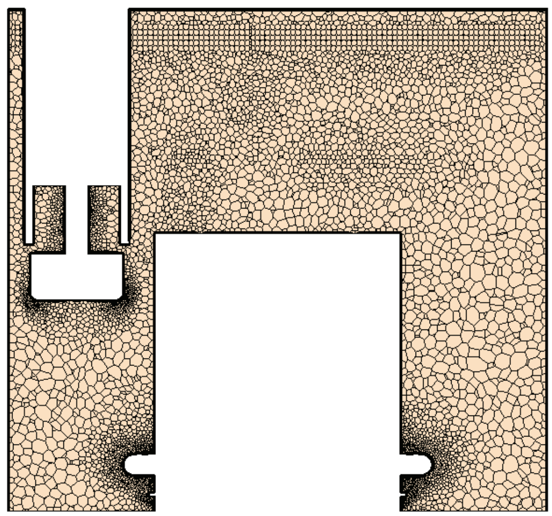

Figure 4. Cold pool mesh

As illustrated in Figure 4, the region of the sodium surface has been refined to better capture the Argon cover gas and sodium region. The mesh has been held considerably small (about 3.5 million cells) in size to quickly receive results during a coupled run. All walls are being considered adiabatic. Therefore influence of near wall discrepancies is considered small. However, as soon as heat is transferred through walls, the mesh should be revised. Results from calculations with larger meshes did not show significant difference.
The volume contains two fluids, liquid sodium [16] (incompressible, but density is dependent on temperature) as coolant and Argonne as compressible cover gas layer. As boundary conditions, the elevation of the sodium surface must be given, the elevation of the pressure boundary as well as its value. Inlet and outlet boundaries are specified by velocity and temperature.
The physics of the two fluids in STAR-CCM+ follow the Eulerian Multiphase model, where each fluid is specified separately. Argonne is specified as ideal gas with constant material properties. Liquid sodium is specified by polynomial functions dependent on density for dynamic viscosity, density and thermal conductivity [16]. Specific heat and speed of sound are assumed constant. Further the Reynolds Averaged Navier Stokes (RANS) approach is used with realizable k-epsilon turbulence model. Gravity is taken into account as it is crucial for natural convection. This model setup is trimmed to save computational efforts.

The simulation is run for 10000s with constant boundary conditions given by the STH simulation in SAS4A/SASSYS-1 to receive developed fields at the beginning of the transient (see Figure 5). Although after approximately 1000s the velocity field did not show significant changes, the temperature field needed about 2500s to fully develop. To have no more influence on any previous initializations and make sure, the field is fully developed, the simulation was run 4 times longer.

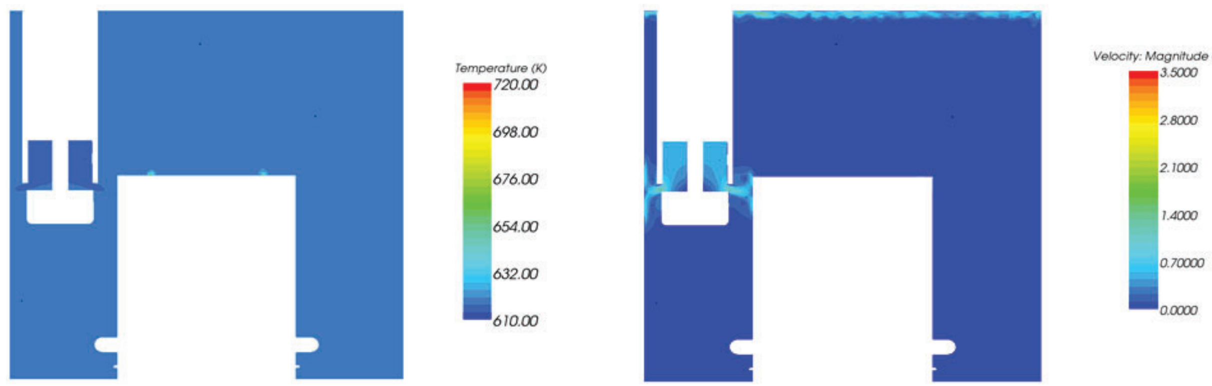

Figure 5. CFD initial fields, temperature [K] (left), velocity magnitude [m/s] (right)

5. Coupling methodology and adaptation

The coupling methodology follows the approach developed by [18] with small modifications, which could be interpreted as *supervised* (both codes are controlled by the coupling interface) *sequential* (codes do exchange parameters sequentially and are therefore run after one another) *explicit* (time step is externally given) overlapping (coupling geometry is in STH and CFD modelled) *coupling*. Modifications to the coupling interface are according to discrepancies in the geometrical description of the EBR-II cold pool in SAS4A/SASSYS-1 and STAR-CCM+. In the STH code, for the leakage of hot sodium, only one region is considered. However, in the physical case, hot sodium enters the cold pool through a small gap between shielding and cover of the core and at the connection of the Z-Pipe to the IHX primary inlet. While running CFD with constant boundary conditions, small discrepancies between inlet mass flowrate and outlet mass flowrate have shown high impact to the simulation's stability and results for steady state. For that reason, the mass balance of sodium is being checked and corrected at the primary pump inlet (considered outlet of the cold pool) by user functions. The assumption here was to keep the mass of sodium in the cold pool constant. User functions in START-CCM+ can be used to perform simple calculations within the CFD simulation run. One example could be the test of another correlation for temperature based density behavior. In that case, temperature can be read from any cell or defined cross-section and the new density can be calculated (and even written out to a file). More information about user function can be found in [9].

Table 1. Association of STAR-CCM+ boundaries and SAS4A/SASSYS-1 liquid segments

STAR-CCM+ Boundary	Boundary type	Corresponding SAS4A/SASSYS-1 segment
Inlet	Inlet	4
Interface	Inlet	14
LowPressurePiping1.leak	Inlet	11
LowPressurePiping2.leak	Inlet	12
OUTLET Pump 1	Inlet	5
OUTLET Pump 2	Inlet	8
Pump1.leak	Inlet	11
Pump2.leak	Inlet	12
Shielding.Top.leak	Inlet	13
Z-Pipe.leak	Inlet	13

Communication between STAR-CCM+ model and SAS4A/SASSYS-1 occurs at the flow boundaries. Each SAS4A/SASSYS-1 segment that is connected to the cold pool volume (CV4) is represented as a flow boundary condition providing mass flow/velocity and enthalpy/temperature to the referring STAR-CCM+ surface. There are 7 flow boundaries in the SAS4A/SASSYS-1 CV4 but 10 flow boundaries in the STAR-CCM+ model. This discrepancy comes from flow boundaries that are associated with relatively low-flow leakage pathways from various pipe junctions into the cold pool. In the 1-D system code representation of the cold pool, these leakage pathways must be placed at either the inlet or outlet of a flow segment, which limits the locations where the leakage pathways can be modeled. In the 3-D CFD model, it is desirable to identify more precise locations for these leakage pathways. Therefore, some of the leakage boundaries in the systems code model are split into multiple boundaries in the CFD model. The relative flow rate for two CFD boundaries associated with a single system code surface is is determined through a ratio calculated from measurements in EBR-II during steady state. The indices for flow boundaries used by the coupling interface are given in Table 1. LowPressurePiping1.leak and Pump1.leak share one SAS4A/SASSYS-1 boundary. As consequence the ratio of mass flow is derived at steady state conditions from measurements. This ratio is kept constant during the whole transient as further information (e.g. pressure loss through leakage area) would be required to calculate it but is not provided during this work. SAS4A/SASSYS-1 provides one value to STAR-CCM+ through the coupling interface in this example. Then, User Field-functions use that value together with the ratio to derive the velocity required at the specified inlet boundary in CFD. These split boundaries in STAR-CCM+ that share one SAS4A/SASSYS-1 value are given in Table 2.

Table 2. Split and merged boundaries between STAR-CCM+ and SAS4A/SASSYS-1

STAR-CCM+ boundary	SAS4A/SASSYS-1 boundary
LowPressurePiping1.leak & Pump1.leak	Segement 11
LowPressurePiping2.leak & Pump2.leak	Segment 22
Shielding.Top.leak & Z-Pipe.leak	Segment 13

6. Benchmark results

Following the CFD initialization described above, coupled simulations were performed for an additional 100 seconds at the steady-state pre-test condition. This simulation time was used to avoid possible initialization discrepancies or numerical oscillations at the beginning of the transient. In the following figures, different simulation results are compared with measurements. For the coupled simulation, the cold pool is represented in CFD. As all walls are considered adiabatic in CFD, the SAS4A/SASSYS-1 model is adjusted and heat transfer through structure walls that touch the cold pool's volume are considered adiabatic as well. For comparison purposes, two STH model versions are shown. One with heat transfer through walls and one without heat transfer through walls touching the cold pool volume. In the following figures, measurements are colored in red, STH without heat transfer to the cold pool are cyan, STH with heat transfer to the cold pool are green and CFD/STH coupled simulation results are blue.

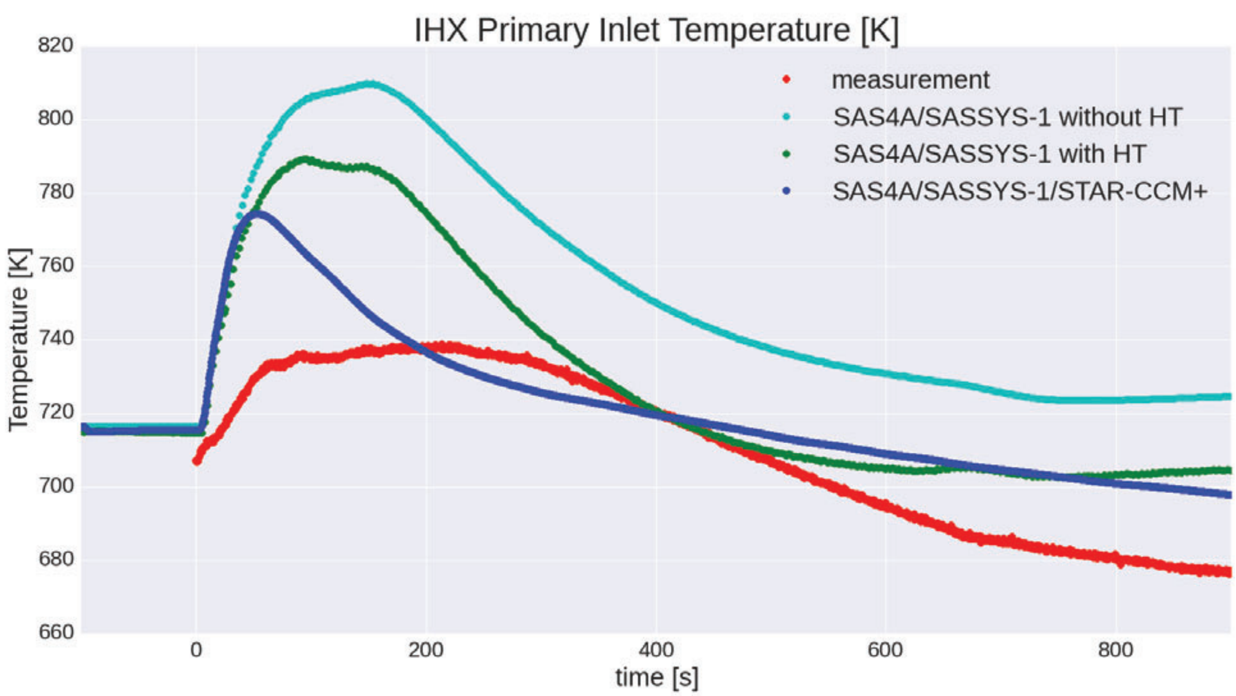

Figure 6. SHRT-45R - IHX primary side inlet temperature [K]

Figure 6 illustrates the temperature curve at the IHX primary side's inlet (end of Z-Pipe). Measurements show increasing temperature behavior during the first 200s of the transient test. Compared to simulations, the measured starting temperature is about 5K smaller than in simulations. This can occur because of averaging in simulations and the thermocouple position. During the first 200s each of the simulations shows sharp increase in temperature. Especially the STH standalone model without heat transfer to the cold pool shows here a very high rise in temperature. Compared with the coupled CFD/STH calculation, where the cold pool is assumed with adiabatic walls, one can see clearly the strong dependency on three-dimensional effects taking place in the cold pool. As the primary pumps' inlet region is of higher elevation than the IHX outlet region, it can be assumed, hot sodium enters the primary pumps more quickly – which is the case in STH standalone. The STH standalone calculation uses heat transfer through walls with a full description of the material where heat is transferred through (conduction). When using heat transfer through walls, heat conduction is modelled with heat transfer correlations.

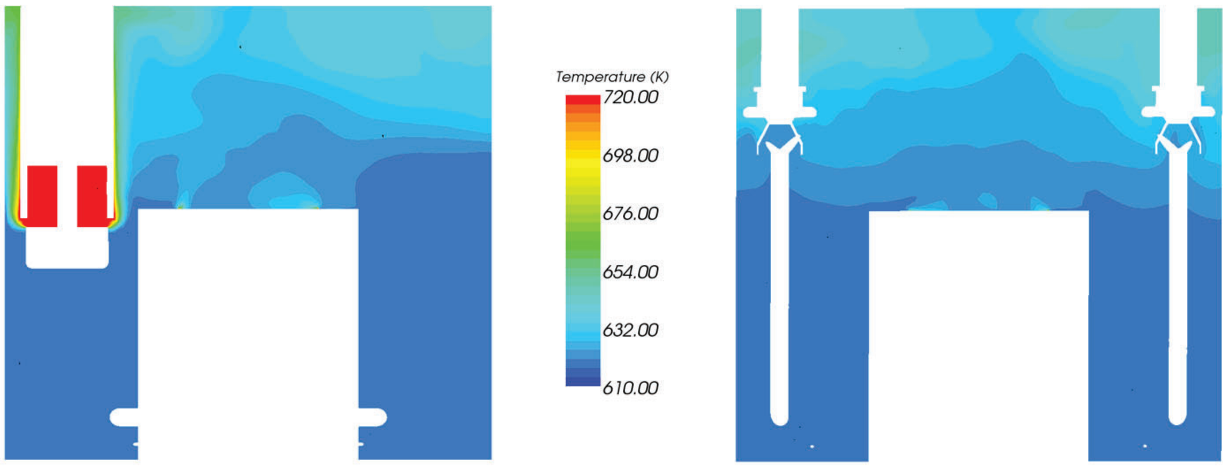

Figure 7. Temperature fields, IHX region (left), Primary pumps region (right)

Figure 7 shows a cross-section of the cold pool with IHX outlet on the left hand side. The boundary field has been transferred into the IHX to avoid artificial (forced) flow behavior at the outlet of the IHX. It can be observed, hot sodium coming out of the IHX travels vertically to the top of the cold pool. In STH codes, large volumes are averaged as total mixing is assumed. This three-dimensional behavior of sodium however can only be captured by coupled CFD/STH solutions. During the transient, it is also visible that heat is stored on top of the cold pool so the temperature of sodium in the core is lower than if the cold pool volume was averaged.

As the SHRT-45R benchmark test is an unprotected loss of flow accident scenario, all sodium flow is only driven by natural circulation. The pump behavior is represented in SAS4A/SASSYS-1 [17] as well as heat generation in the core. In the cold pool of the EBR-II reactor, two rows of thermos couples have been installed to measure temperatures at different elevations. One of these is called F-Probes. The position has been approximated in the CFD cold pool model. The temperature over time clearly shows thermal stratification (Figure 8) in the CFD calculation which cannot be shown in STH as control volumes are very large. In Figure 7 on the left hand side, the temperature field is shown at the position of the IHX right after the pump trip. It can be observed, that hot sodium entering the cold pool from the IHX vertically travels to the top (sodium surface). The primary pumps still are fed with cold sodium. As STH simulations assume total mixing in a control volume, this practically shows the importance of a CFD representation of the cold pool and therefore a coupled solution of the transient scenario. It can also be observed that at the end of the transient, the temperature difference gets smaller again. As shown before in Figure 7, the highest temperatures are ‘stored’ at high elevations of the cold pool (sodium and Argonne) and then get lower as the cold pool starts to heat up but cannot be compared to total mixing.

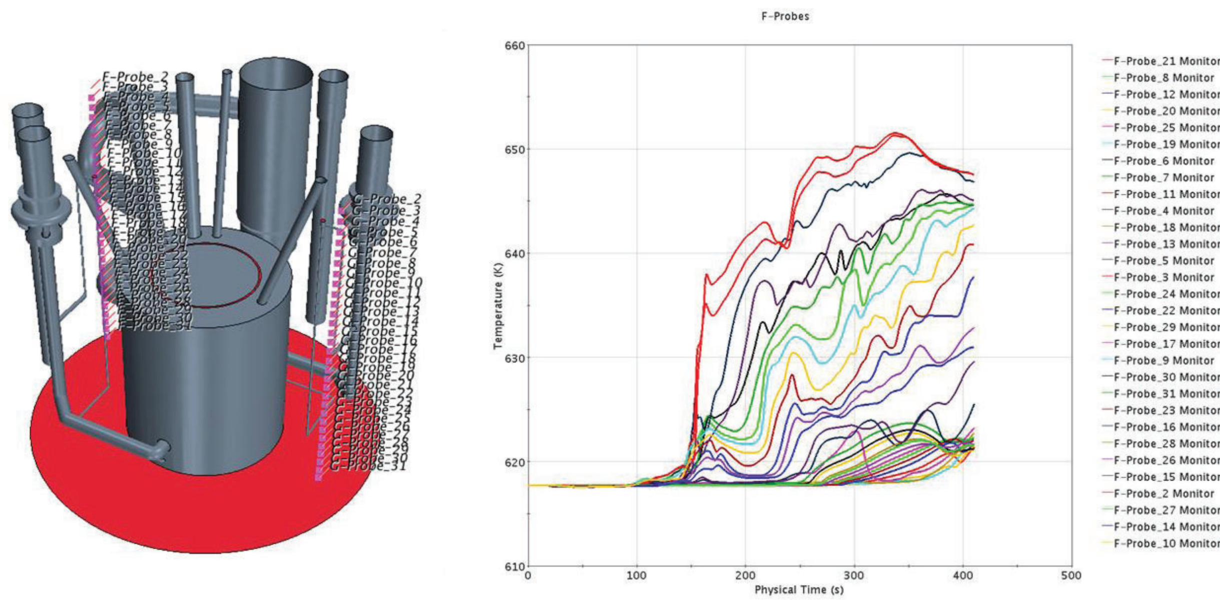

Figure 8. Position of thermal couples in cold pool (left) , Temperature at individual position [K] (right)

However, during the assessment of the coupled simulation, some strong discrepancies in temperature occurred that cannot be explained with thermal stratification of other thermal behavior of the cold pool. For that reason, the mass flow rates have been evaluated. Here, the Z-Pipe was taken as a comparison between STH standalone and coupled simulations. It occurred, that the mass flow rate in coupled simulation was significantly higher predicted than in STH standalone. With this in mind, the high outlet temperature at the IHX outlet region from the coupled simulation can be explained.

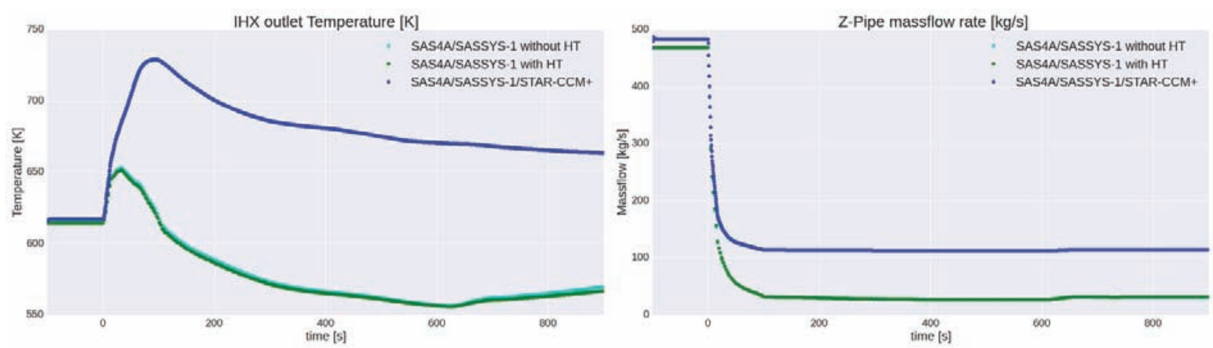

Figure 9. IHX outlet temperature [K] (left) and Z-Pipe mass flow rate [kg/s] (right)

7. CONCLUSIONS

The SHRT-45R benchmark test shows high potential for coupled simulations as well as for STH code qualifications. As it is an unprotected loss-of-flow accident scenario starting at full power. The CFD model has been developed with complex geometries that penetrate the cold pool volume. That way, free flow stream behavior cannot be assumed anymore but more complex flow structures take place. For the natural circulation case during the transient, it was shown that CFD has higher potential to predict complex flow and thermal behavior. To have a feedback to the rest of the primary circuit, CFD (STAR-CCM+) was coupled to STH (SAS4A/SASSYS-1) with a previously developed but slightly modified methodology. The coupled results showed preliminary good quality and the stability of the coupling methodology was given at all times. However, more work in this field is necessary to reach higher flexibility in the coupling interface (e.g. heat transfer through walls) and further investigations due to discrepancies in mass flow rate are due.

ACKNOWLEDGMENTS

This work was done during an internship at Argonne National Laboratory (ANL). I want to thank Prof. X. Cheng (KIT) and T. Sofu (ANL) for their efforts. For the support of my work and great supervision, I want to thank J.W. Thomas (ANL) as well as T. Sumner (ANL) and T.H. Fanning for his insides and support with the STH code.

REFERENCES

1. **Generation IV International Forum.** The Generation IV International Forum. *The Generation IV International Forum.* [Online] 2014. [Cited: March 2, 2015.] https://www.gen-4.org/.
2. *Use and Development of Coupled Computer Codes for the Analysis of Accidents at Nuclear Power Plants.* **International Atomic Energy Agency (IAEA).** Vienna : IAEA, 2003. IAEA-TECDOC-1539.
3. **Petruzzi, Alessandro and D'Auria, Francesco.** Thermal-Hydraulic System Codes in Nulcear Reactor Safety and Qualification Procedures. *Science and Technology of Nuclear Installations.* November 8, 2007.
4. **Levy, Salomon .** The important role of thermal hydraulics in 50 years of nuclear power applications. *Nuclear Engineering and Design.* September 1, 1994, pp. 1–10.
5. **Tenchine, D.** Some thermal hydraulic challenges in sodium cooled fast reactors. *Nuclear Engineering and Design.* May 5, 2010, pp. 1195–1217.
6. **Chellapandi, P., Chetal, S.C. and Raj, Baldev.** Thermal striping limits for components of sodium cooled fast spectrum reactors. *Nuclear Engineering and Design.* December 2009, pp. 2754–2765.
7. **Golden, G.H., et al., et al.** Evolution of thermal-hydraulics testing in EBR-II. *Nuclear Engineering and Design.* April 1987, pp. 3-12.
8. *Advanced LMR Safety Analysis Capabilities in the SASSYS-1 and SAS4A Computer Codes.* **Cahalan, J.E., Tentner, A.M. and Morris, E.E.** [ed.] American Nuclear Society. Pittsburgh : American Nuclear Society, 1994. Proc. of the International Topical Meeting on Advanced Reactors Safety. Vol. 2, pp. 1038–1045.
9. **CD-adapco.** STAR-CCM+ v8.04. Melville, NY : s.n., 2013.
10. **Sackett, J.I.** Operating and test experience with EBR-II, The IFR Prototype. *Progress in Nuclear Energy.* 1997, 2, pp. 111-129.
11. **Koch, Leonard J.** *Experimental Breeder Reactor-II (EBR-II) - An Integrated Experimental Fast Reactor Nuclear Power Station.* s.l. : American Nuclear Society (ANS), 2008. ISBN: 0-89448-042-1.
12. **Sherman, Steven R. and Knight, Collin J.** Post-Operational Treatment of Residual Na Coolant in EBR-II Using Carbonation. [book auth.] Pavel Tsvetkov. *Nuclear Power - Deployment, Operation and*

Sustainability. http://www.intechopen.com/books/nuclear-power-deployment-operation-and-sustainability/post-operational-treatment-of-residual-na-coolant-in-ebr-ii-using-carbonation : InTech, 2011.
13. **Mohr, D., et al., et al.** Loss-of-primary-flow-without-scram tests: Pretest predictions and preliminary results. *Nuclear Engineering and Design.* April 1987, S. 45–56.
14. **Planchon, H.P., et al., et al.** Implications of the EBR-II inherent safety demonstration test. *Nuclear Engineering and Design.* April 1987, S. 75–90.
15. **Argonne National Laboratory (ANL).** SAS. *SAS.* [Online] 6. March 2013. [Zitat vom: 3. March 2015.] https://wiki.anl.gov/sas.
16. **Fanning, T. H., ed.** *The SAS4A/SASSYS-1 Safety Analysis Code System.* s.l. : Nuclear Engineering Division, Argonne National Laboratory, 2012. ANL/NE-12/4.
17. *Simulations of the EBR-II Tests SHRT-17 and SHRT-45R.* **Sumner, T. und Moisseytsev, A.** Chicago : s.n., to be published in August 2015. Proceedings of NURETH-16.
18. *Validation of the Integration of CFD and SAS4A/SASSYS-1: Analysis of EBR-II Shutdown Heat Removal Test 17.* **Thomas, J.W., et al., et al.** Chicago : s.n., 2012. Proceedings of ICAPP'12. 12338.